

Monthly Variations of Low-Energy Ballistic Transfers to Lunar Halo Orbits

Jeffrey S. Parker*

The characteristics of low-energy transfers between the Earth and Moon vary from one month to the next largely due to the Earth's and Moon's non-circular, non-coplanar orbits in the solar system. This paper characterizes those monthly variations as it explores the trade space of low-energy lunar transfers across many months. Mission designers may use knowledge of these variations to swiftly design desirable low-energy lunar transfers in any given month.

Nomenclature

τ	Location about a libration orbit, deg
ΔV	Change in velocity, km/s
BLT	Ballistic Lunar Transfer
C3	Injection Energy, km^2/s^2
ET	Ephemeris Time
LEO	Low Earth Orbit
RA	Right Ascension
RAV	Right Ascension of the Apogee Vector
DAV	Declination of the Apogee Vector
L_1	The Lagrange point between the two primary bodies
L_2	The Lagrange point on the far side of the smaller primary body
EL_i	A Sun-Earth Lagrange point
LL_i	An Earth-Moon Lagrange point
T_{ref}	Reference epoch for a three-body orbit

I. Introduction

Low-energy transfers to the Moon have been receiving increased attention in recent years due to their flexibility and potential to reduce the fuel requirements for spacecraft compared with conventional, 3–6 day direct lunar transfers. The two Artemis spacecraft are currently traveling to the Moon via low-energy lunar transfers in such a way that they do not require any large insertion maneuver to become captured by the Moon.¹ The spacecraft do not have the capability to perform direct, Hohmann-like lunar transfers, but they are indeed able to transfer to the Moon via low-energy transfers. This is in part made possible because both Artemis spacecraft will enter libration orbits when they arrive at the Moon.

Many authors have studied how to build low-energy lunar transfers.^{2–12} The majority of work has demonstrated that transfers may be constructed via a sequence of targeting. In previous papers we have demonstrated how to construct and analyze low-energy ballistic transfers using dynamical systems theory.^{3–5,13,14} This method reveals entire families of low-energy transfers, where the parameters of a lunar transfer vary continuously from one end of the family to the other. In a hypothetical system where the motion of a spacecraft is driven only by the gravity of the Sun, Earth, and Moon, and those bodies orbit their respective barycenters in circular coplanar orbits, then a spacecraft can launch onto geometrically identical low-energy transfers each synodic month. The motion of the Earth, Moon, and Sun in the real solar system are not

*Member of Technical Staff, Jet Propulsion Laboratory, California Institute of Technology, M/S 301-121, 4800 Oak Grove Dr., Pasadena, CA 91109, AIAA Member

circular or coplanar, and other perturbations exist; hence, low-energy transfers vary in their characteristics from one synodic month to the next. The research presented in this paper studies these variations in order to identify which types of transfers exist in each month, which appear only in certain months, and how predictable a family of transfers is from month to month.

I.A. Low-Energy Ballistic Lunar Transfers

The low-energy ballistic transfers (BLTs) presented in this paper are trajectories that transfer between the Earth and the Moon and take advantage of the Sun’s gravity to reduce the fuel requirements of the spacecraft. Low-energy transfers typically require 100 or more days to perform, but require on the order of 15% less ΔV than conventional Hohmann-like lunar transfers. The ΔV reduction is very significant if the spacecraft is transferring to or from a lunar libration orbit. Two example ballistic lunar transfers are illustrated in Figure 1, shown in the Sun-Earth rotating frame from above the ecliptic. A spacecraft traversing such low-energy transfers typically travels 1–1.5 million kilometers away from the Earth toward either the Sun-Earth L_1 or L_2 points before falling back to its perigee. The transfer may be compared with a bi-elliptic transfer, where the Sun performs the intermediate maneuver at the spacecraft’s apogee.

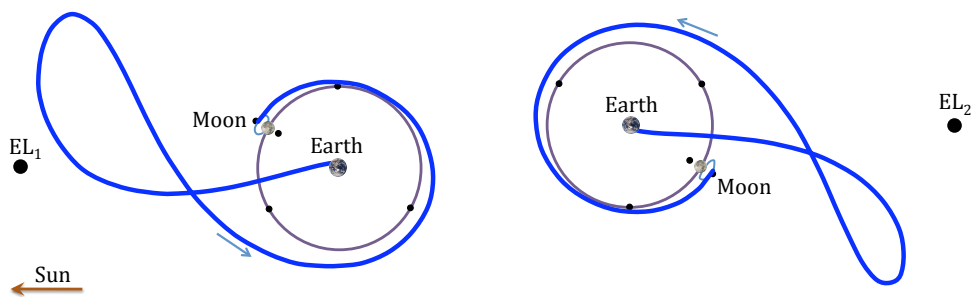


Figure 1. Two dynamical systems ballistic lunar transfers, viewed in the Sun-Earth rotating frame from above the ecliptic.

A spacecraft that uses a low-energy transfer to arrive at a lunar libration orbit, such as a halo orbit, does not require a large orbit insertion maneuver. The trajectory may be constructed such that it asymptotically arrives at the orbit and inserts naturally. Figure 2 illustrates an example of this asymptotic arrival into a lunar libration orbit. More details of these transfers may be found in References 3 – 5.

Studies have also been conducted to understand how to build a practical low-energy lunar transfer with realistic mission constraints.¹⁵ The research indicates that it requires on the order of 50 m/s of ΔV to build a 21 day launch period, and roughly 1 m/s per degree of inclination needed to correct a ballistic lunar transfer to depart the Earth from a particular orbit, such as one with an inclination of 28.5° .

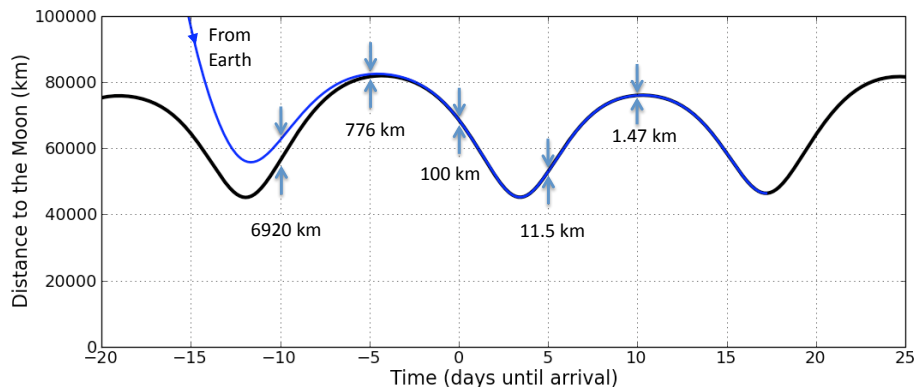


Figure 2. The distance between the Moon and a spacecraft as the spacecraft approaches a target lunar libration orbit.

I.B. The Dynamical Systems Method

Previous papers have demonstrated how to use dynamical systems theory to construct and analyze low-energy transfers between low-Earth orbits and the Moon.^{2-6,13,14} The process takes advantage of the dynamics of the invariant manifolds of unstable orbits that exist in the Sun-Earth and Earth-Moon three-body systems, particularly those orbits around the collinear Lagrange points of each system.

A mission designer first selects an unstable lunar libration orbit to target; it may be selected for its own purposes, e.g., as a navigation, mapping, or science orbit, or as a staging orbit before transferring to another orbit. The mission designer then generates the libration orbit's stable manifold, namely, the set of trajectories that a spacecraft could take to asymptotically arrive onto that orbit. As the trajectories in the orbit's stable manifold are propagated backward in time, they quickly depart the vicinity of the Moon and enter space that is dominated by the gravitational force of the Sun and Earth. The designer then identifies a trajectory that traverses this area in space and eventually falls toward the Earth. This process is illustrated in Figure 3. By adding one or two small maneuvers, the designer can connect the stable manifold with a particular low Earth orbit, such as one with an inclination of 28.5° .¹⁵

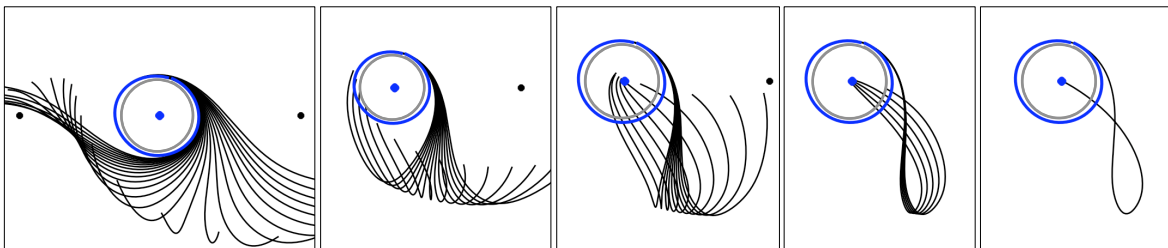


Figure 3. An illustration of the process of selecting a trajectory in a lunar libration orbit's stable manifold that intersects the Earth when propagated backward in time. The trajectories are shown in the Sun-Earth rotating coordinate frame from above the ecliptic.

I.C. Families of Transfers

Dynamical systems methods provide the means to identify families of transfers. A particular low-energy transfer has a set of performance parameters, including its Earth departure time, departure geometry, transfer duration, arrival time, etc. Previous studies have demonstrated how to construct a low-energy transfers from a 185 km LEO parking orbit to a specific lunar libration orbit using just two targeting parameters: T_{ref} and τ , which define the time of arrival at the Moon and the location of the arrival point about the target libration orbit.^{3,13,14} If one perturbs the value of one of these parameters, it is often the case that one can find a new value for the other parameter that achieves a new lunar transfer. One can trace out curves in the state space of these two parameters such that each combination of the two parameters in the curve yields the initial state of a trajectory that intersects a 185 km LEO parking orbit when propagated backward in time. Figure 4 shows an example of such a state space map. A trajectory is generated for every combination of T_{ref} and τ and the closest perigee passage is recorded in the map. The curves colored black correspond to those combinations of the two parameters that yield low-energy lunar transfers that originate from low Earth orbits.

Every performance parameter of the transfers in a family varies in a continuous fashion from one end of the family to the other. Figure 5 shows examples of the shapes and features of these transfers and where they exist in the state space map. Most of the transfers identified in the state space map depart the Earth with a launch energy in the range of $-0.75 \text{ km}^2/\text{s}^2 \leq C3 \leq -0.35 \text{ km}^2/\text{s}^2$ and do not traverse any Earth phasing orbits or lunar flybys.⁵ It has been observed that a lunar flyby on the outward leg with a perilune altitude of approximately 2000 km may reduce the required launch energy to a value near $-2.1 \text{ km}^2/\text{s}^2$.⁵

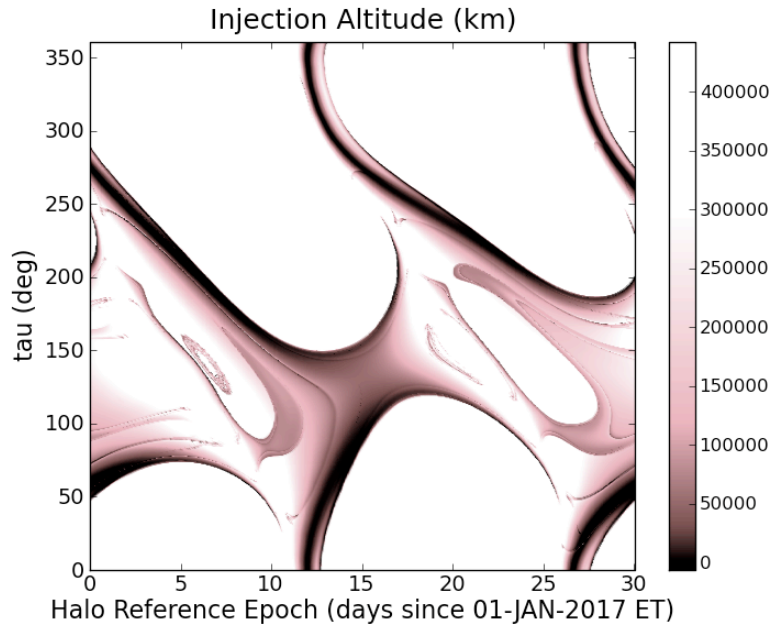


Figure 4. An example state space map that shows the injection altitude for low-energy ballistic lunar transfers as a function of their arrival date at the Moon and arrival location, τ , about their target lunar orbit.

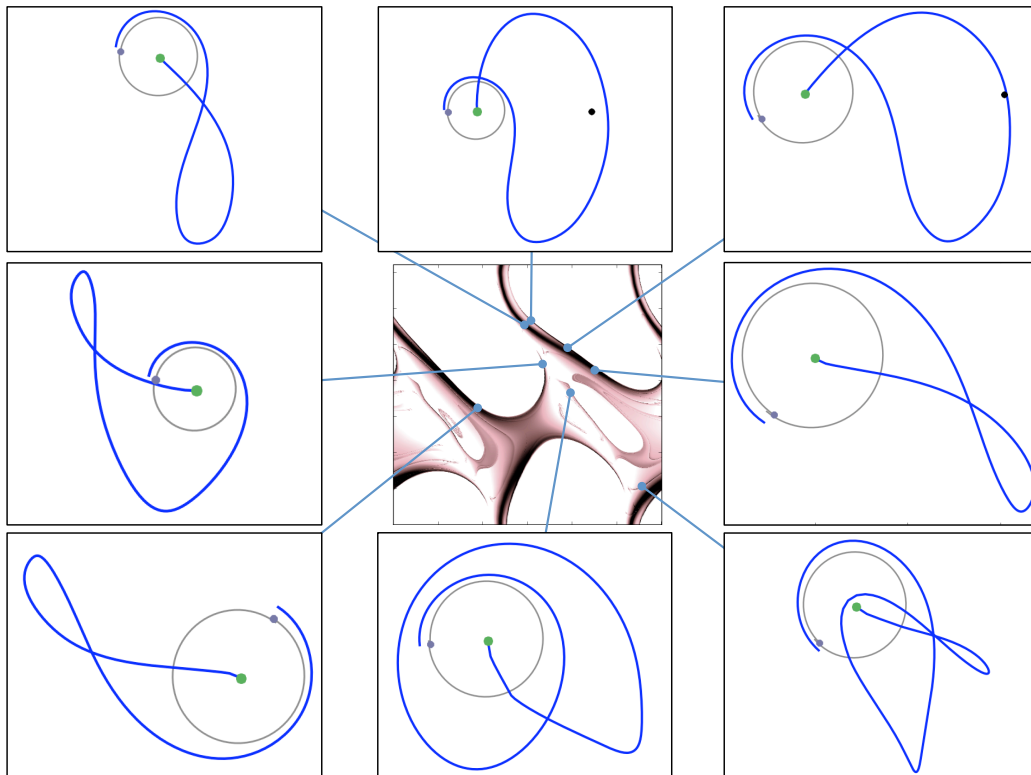


Figure 5. The state space map shown in Figure 4 reveals a wide variety of different low-energy ballistic lunar transfers, each of which exists in a family of similar trajectories.

I.D. Implementation

The research presented in this paper is a continuation of the research presented in Reference 5. The low-energy transfers are constructed in the same manner and the same lunar libration orbit is being targeted. This method will be briefly described here.

The target libration orbit is a quasi-halo orbit about the Earth-Moon L_2 point. Halo orbits are periodic in the circular restricted three-body problem (CRTBP);^{16,17} they become quasi-periodic in the real solar system due to realistic perturbations, such as the Moon's non-circular orbit.¹⁸ The specific quasi-halo orbit being targeted has been generated by differentially correcting a perfectly periodic halo orbit from the CRTBP into a realistic model of the solar system.^{16,19,20} The target orbit is a Southern halo orbit about the Earth-Moon L_2 point with a z -axis amplitude of 30,752 km (0.08 normalized distance units). The reference time for the differential correction process varies for the specific transfer, but is near January 1, 2017. The JPL DE421 Planetary and Lunar Ephemerides²¹ has been used as the model of the solar system. Figure 6 shows an illustration of the resulting quasi-halo orbit that is being targeted.

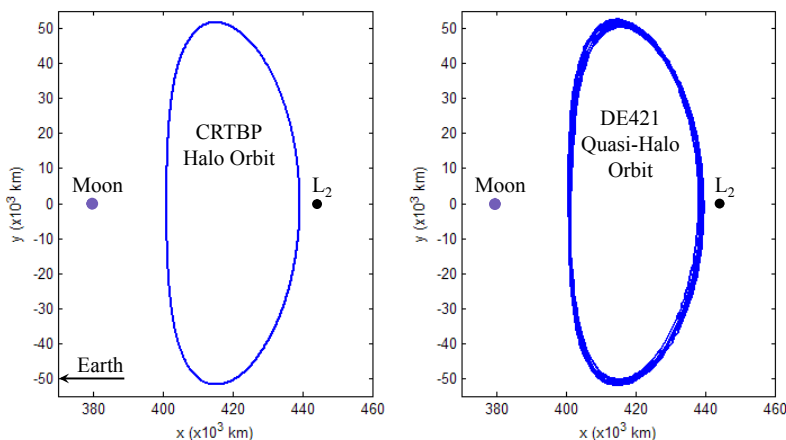


Figure 6. A comparison of the perfectly periodic reference halo orbit generated in the CRTBP (left) with the quasi-halo orbit differentially corrected in the DE421 ephemeris model of the solar system (right). The trajectories are viewed in the Earth-Moon rotating coordinate frame from above the ecliptic.

Two parameters are varied to trace out families of low-energy lunar transfers. The first is the reference epoch of the quasi-halo orbit, T_{ref} . The reference epoch defines the location of the Moon at the time of arrival. The second parameter is the arrival location, τ , where the spacecraft injects into the libration orbit. Since the trajectory asymptotically arrives at the orbit the spacecraft does not need to perform an injection maneuver; the injection is defined arbitrarily as the location in the orbit when the spacecraft has approached to 100 km of the orbit. The parameter τ is analogous to a conic orbit's true anomaly: it has a value of 0° where the orbit crosses the Earth-Moon syzygy axis with positive y -velocity and it increases at a constant rate over time until it reaches a value of 360° at the next positive y -velocity syzygy axis crossing. Since the quasi-halo orbit is not perfectly periodic, each orbital revolution requires a slightly different amount of time. Thus, τ increases at a slightly different rate from one revolution about the orbit to the next.

The state space map shown in Figures 4 and 5 has been generated using the procedure described here.

II. Monthly Variations

The process used to generate the state space map that is shown in Figures 4 and 5 has been extended in this paper, studying how it varies from month to month. Figure 7 shows the state space map extended over three months. One can see that the state space map clearly varies from one month to the next, although the most prominent features repeat regularly.

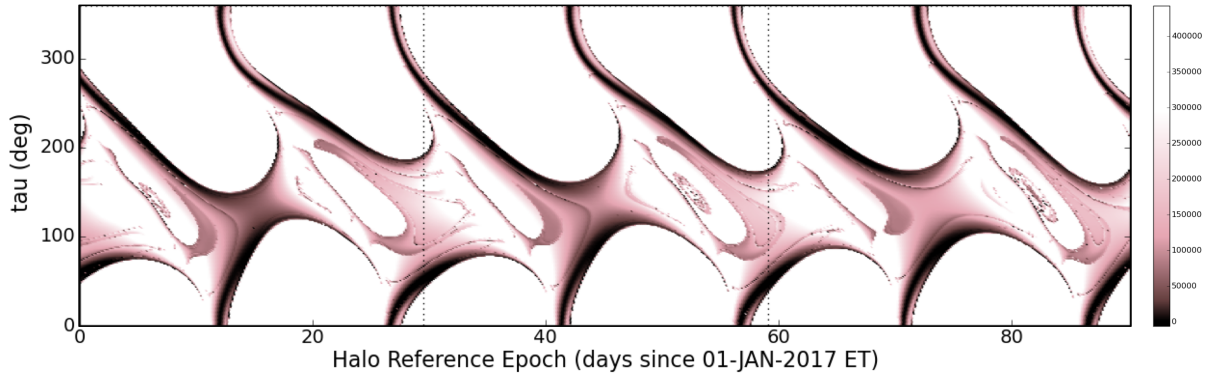


Figure 7. The state space map shown in Figure 4 extended for three months.

II.A. 12 Month Survey

The state space map has been further extended to 12 months to study the variations that exist throughout an entire year. It has been observed that the most prominent features continue to persist, and repeat regularly, while subtle features appear and disappear from month to month. The 185-km curves in the full 12 months have been traced out throughout the map to generate families of low-energy lunar transfers. Figure 8 shows a plot of samples of the combinations of T_{ref} and τ that yield low-energy transfers between 185 km LEO parking orbits and the lunar halo orbit.

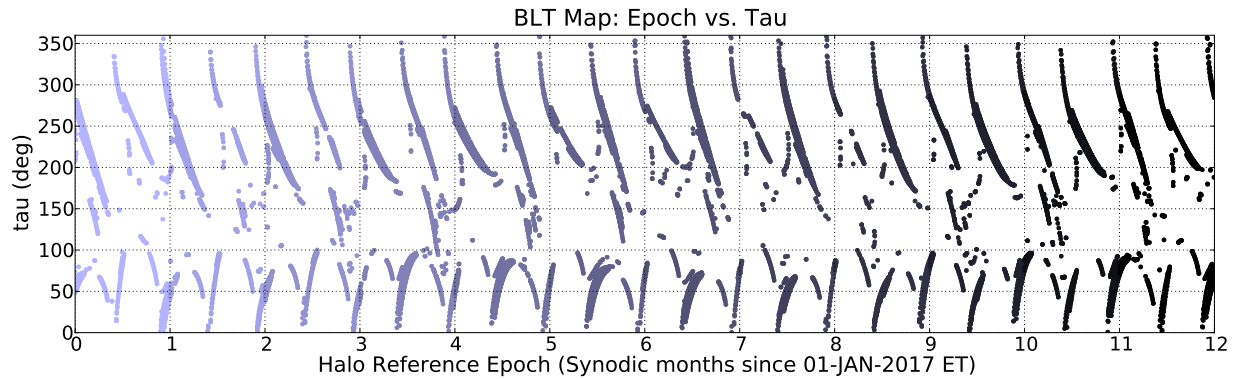


Figure 8. Sample combinations of T_{ref} and τ that yield low-energy transfers between 185 km LEO parking orbits and the lunar halo orbit for reference dates that span the year 2017.

The reference epoch of each transfer shown in Figure 8 may be wrapped into one synodic month to observe the changes that occur in the state space map from one synodic month to the next. Figure 9 shows the resulting plot, revealing the variations in the locations of the curves as they shift throughout the 12 months. The transfers are shaded in Figure 9 in the same manner as they are in Figure 8, i.e., the transfers that exist in the first month, which starts at a reference epoch of Jan 1, 2017, are shown in the lightest shade and the transfers in each consecutive synodic month thereafter are plotted in a darker shade. One can see that certain features repeat very closely from one synodic month to the next. Other features only appear in a subset of synodic months.

Quite a few patterns exist in the families of transfers that are observed. First of all, the most pronounced curves observed in Figures 8 and 9 correspond to transfers that do not include any lunar flybys or Earth phasing orbits. Most of them require between 90 and 110 days to transfer between the Earth and 100 km from their target orbit. Examples of these sorts of transfers may be seen in Figure 5.

Several relationships exist between the launch energy of a low-energy lunar transfer and how close it gets to the Moon on its Earth-departure leg. If the transfer does not encounter the Moon, it typically requires a

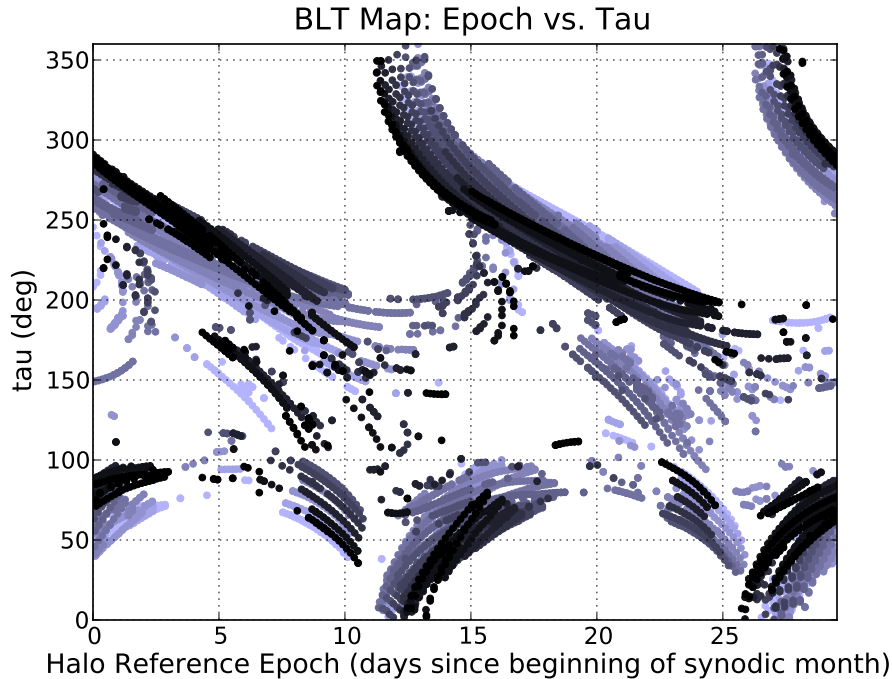


Figure 9. The combinations of T_{ref} and τ that yield low-energy lunar transfers during 12 synodic months, relative to the beginning of each synodic month. The first month, which starts at a reference epoch of 1 Jan 2017 00:00:00 Ephemeris Time, is shown in the lightest shade and each consecutive month thereafter is plotted in a darker shade.

launch energy in the range of $-0.75 \text{ km}^2/\text{s}^2 \leq C3 \leq -0.35 \text{ km}^2/\text{s}^2$. If a spacecraft traversing a low-energy transfer does encounter the Moon as it departs the Earth's vicinity, one finds that the Moon may either boost or reduce the spacecraft's energy, depending on how the spacecraft passes by the Moon. If it boosts the spacecraft's energy, then the lunar transfer's required launch energy drops to as low as $-2.1 \text{ km}^2/\text{s}^2$. Figure 10 shows a plot of the relationship between the launch energy of each low-energy transfer observed in Figure 9 and how close the transfer passes by the Moon.

One can also glean a great deal of understanding about the characteristics of these transfers by observing the relationship between each transfer's injection energy and the transfer's duration. Figure 11 shows this relationship for each transfer in the 12 month survey. One can see that the trends in this relationship are nearly independent of the month of the transfer. Typical mission designs prefer the transfer duration to be as short as possible. One can see that there are two types of transfers that require fewer than 100 days to perform: those that require an injection $C3$ on the order of -2.1 to $-1.5 \text{ km}^2/\text{s}^2$ and those that require an injection $C3$ on the order of -0.7 to $-0.5 \text{ km}^2/\text{s}^2$. Clearly, those that require less injection $C3$ pass near the Moon on the way out of the Earth's vicinity.

The *inertial* orientation of each low-energy transfer observed in this 12 month survey clearly depends on which month the transfer departs the Earth. However, the orientation of each similar low-energy transfer is fairly constant throughout the year when observed in the Sun-Earth rotating frame. One way to observe that is to track each transfer's departure from Earth in the Sun-Earth rotating frame. Figure 12 shows a plot that compares the departure state of each transfer in the 12 month survey by plotting the relationship of each transfer's RAV and DAV parameters, namely, the right ascension and declination of the transfer's initial apogee vector. The RAV and DAV values have been computed at the instant of the trans-lunar injection, before any perturbations change the orbit. Each transfer departs the Earth on an orbit that is highly eccentric, but still captured by the Earth. From Figure 12, one can see that this initial orbit is usually oriented near the ecliptic plane and usually oriented either toward or away from the Sun. A RAV value of 0° corresponds to an orbit that has its apogee vector pointing away from the Sun, in the direction of positive x in the Sun-Earth rotating coordinate frame.¹⁷ The outlying points in the figure correspond to transfers that include some combination of Earth phasing loops and lunar flybys and typically do not reappear in the same region of this figure from one month to the next.

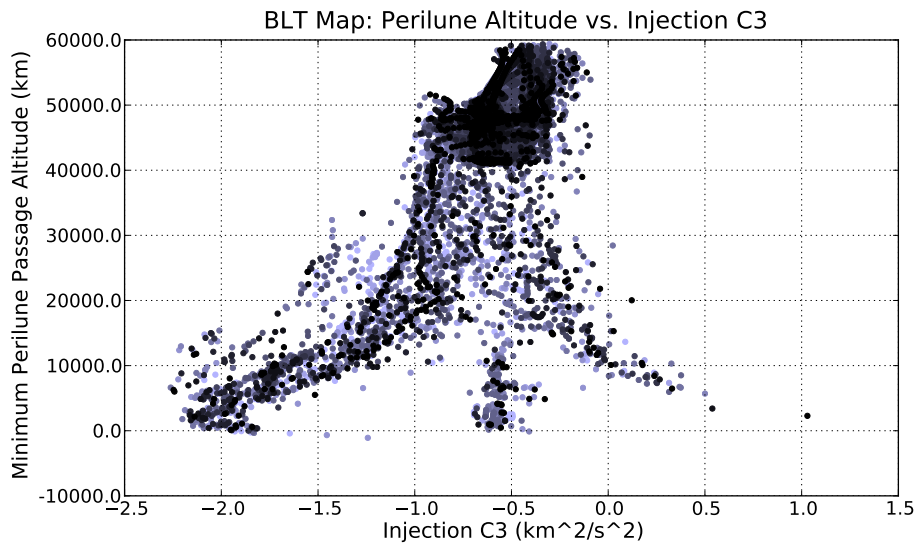


Figure 10. The relationship between injection C3 and the lowest perilune altitude for each transfer in the 12 month survey. The trajectories near the top of the plot do not include any lunar flyby; trajectories toward the bottom do, where those toward the bottom-left receive an energy boost from the Moon and those toward the bottom-right have energy removed by the Moon.

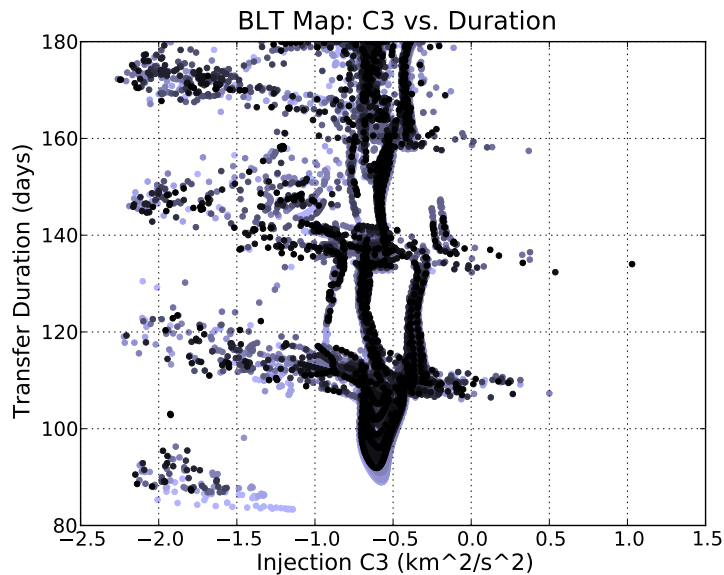


Figure 11. The relationship between injection C3 and duration for each transfer in the 12 month survey.

II.B. Tracking a Family Through 12 Months

Previous studies have shown that one can trace hundreds of different families of low-energy lunar transfers in any given reference month.³ The characteristics of these families often stack on top of each other in each relationship presented in Figures 9–12, making it difficult to discern how the characteristics of one family evolve from month to month. The present study has filtered the set of low-energy transfers in the 12-month survey to attempt to isolate a particular set of practical low-energy transfers. It is often the case that a practical spacecraft mission benefits by shorter transfer durations. It is also usually beneficial to avoid outbound lunar flybys because they add geometrical constraints to the system that make it more difficult to

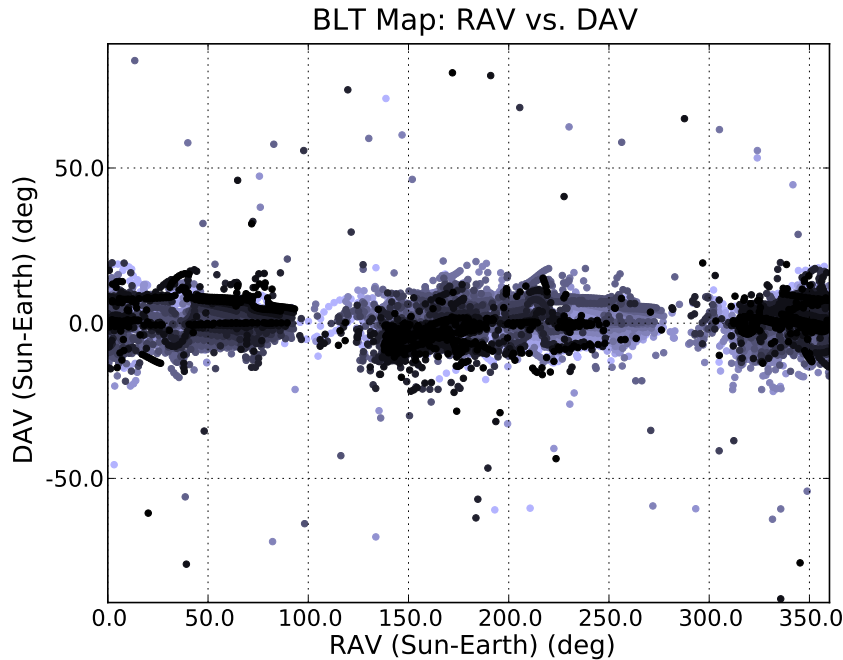


Figure 12. The relationship between the right ascension and declination of the apogee vector, RAV and DAV, respectively, for each transfer in the 12 month survey.

establish a wide launch period. Hence, the filters that have been applied include:

- Maximum duration: 105 days
- Minimum perilune altitude: 20,000 km

In addition, the set of all transfers that meets these criteria has been divided into two subsets, split such that one subset includes those transfers that travel closer to EL_1 than EL_2 and vice versa. In this way, one can compare practical EL_1 transfers in each month and practical EL_2 transfers from one month to the next.

Figure 13 identifies the transfers that meet the filter criteria in the state space map. A visual comparison will confirm that these transfers exist in the most prominent features of the state space maps shown in Figures 4, 5, 8, and 9. One can see that the location of the curves of each family on these plots varies from month to month; the variations appear to be contained within approximately 50 deg in τ and at most 5 days in the orbit's reference date, T_{ref} .

Figure 14 shows the relationship of each transfer's injection C3 and its duration for every transfer that satisfies the filter criteria. One can clearly see that the transfers' performance parameters vary along a curve for each month, and the performance curve does not vary significantly from one month to the next: the transfer duration may vary by several days between months, but the curves span very similar ranges of injection C3.

It is very interesting to plot the relationship between each transfer's injection date and its injection energy, C3. Figure 15 shows this comparison for the EL_1 and EL_2 transfers. One can see that the families of transfers shift on this plot from month to month. The comparison also shows that most families of transfers span an injection date of 10 to 15 days. This suggests that there are 10 to 15 days in a launch period to this lunar libration orbit via this type of transfer before the deep space ΔV cost increases. This relationship, however, does not take into account differences in the injection inclination throughout the family. Figure 15 also verifies that EL_1 transfers and EL_2 transfers depart approximately two weeks apart from each other.

The departure geometry of the filtered transfers is very consistent and predictable from month to month, given the proper analysis. Figures 16 and 17 show the RAV and DAV parameters for the EL_1 and EL_2 transfers, respectively, computed in the Sun-Earth rotating coordinate frame at the instant of trans-lunar injection. One can immediately observe that the ranges of RAV and DAV values are very limited for each

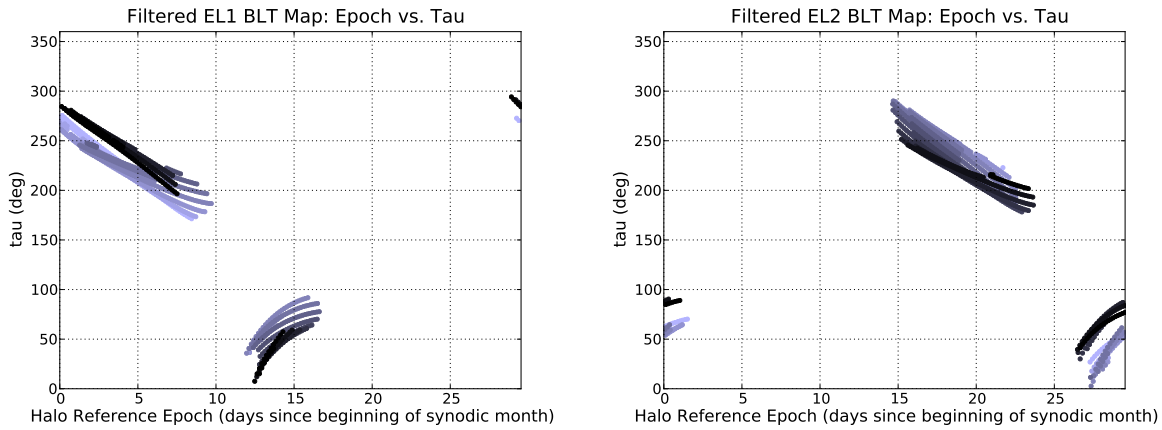


Figure 13. The relationship between the reference epoch and τ for each EL_1 (left) and EL_2 (right) transfer in the 12 month survey that satisfies the filter criteria.

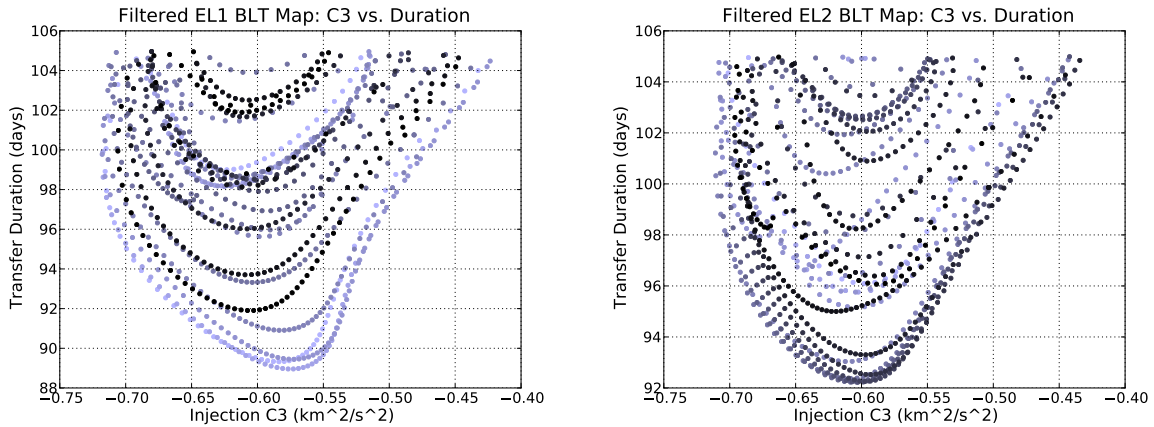


Figure 14. The relationship between the injection C3 and transfer duration for each EL_1 (left) and EL_2 (right) transfer in the 12 month survey that satisfies the filter criteria.

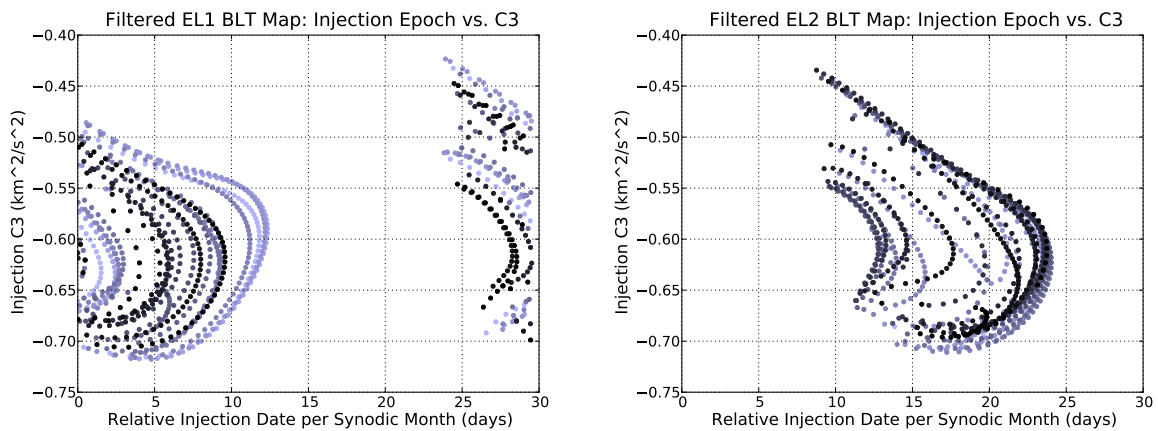


Figure 15. The relationship between the injection date and the injection C3 for each EL_1 (left) and EL_2 (right) transfer in the 12 month survey that satisfies the filter criteria.

set of transfers: the EL_1 transfers are confined to the approximate range $\sim 140^\circ \leq RAV \leq \sim 170^\circ$, the EL_2 transfers are confined to $\sim 320^\circ \leq RAV \leq \sim 355^\circ$, and both sets are confined in DAV to the approximate range $\sim -10^\circ \leq DAV \leq \sim 10^\circ$. The RAV values appear to cover a very similar span of values for each month, but there appears to be an annual signal in the DAV values. This systematic variation may be isolated by observing the relationship between a transfer's DAV value and the orientation of the Moon's orbital pole vector at the arrival time. The Moon's orbit has an inclination of approximately 5.1° relative to the ecliptic. The Moon's orbital plane is approximately fixed in inertial space, but rotates in the Sun-Earth rotating frame. Figure 18 shows the relationship between the transfer's injection DAV value and the right ascension of the lunar orbit pole vector in the Sun-Earth rotating coordinate frame at the time of arrival. One sees a clear annual signal in the data. A mission designer may be able to use this information to improve an initial estimate of the trans-lunar injection geometry. The injection DAV value still varies by approximately 10 degrees throughout a family after accounting for the annual variation. This remaining variation may be explained by the z -axis motion of the target orbit at the time of arrival, though that relationship has not been studied sufficiently yet.

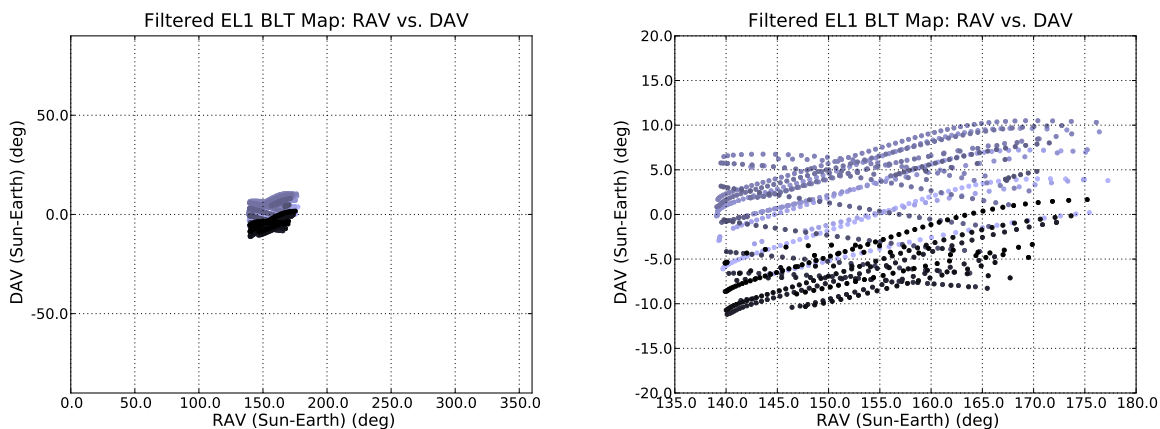


Figure 16. The relationship between RAV and DAV (the right ascension and declination of the apogee vector) at the time of trans-lunar injection for the filtered EL_1 transfers. Left: one can see that RAV and DAV are confined in a narrow box for these transfers; Right: a closer look at the parameter space.

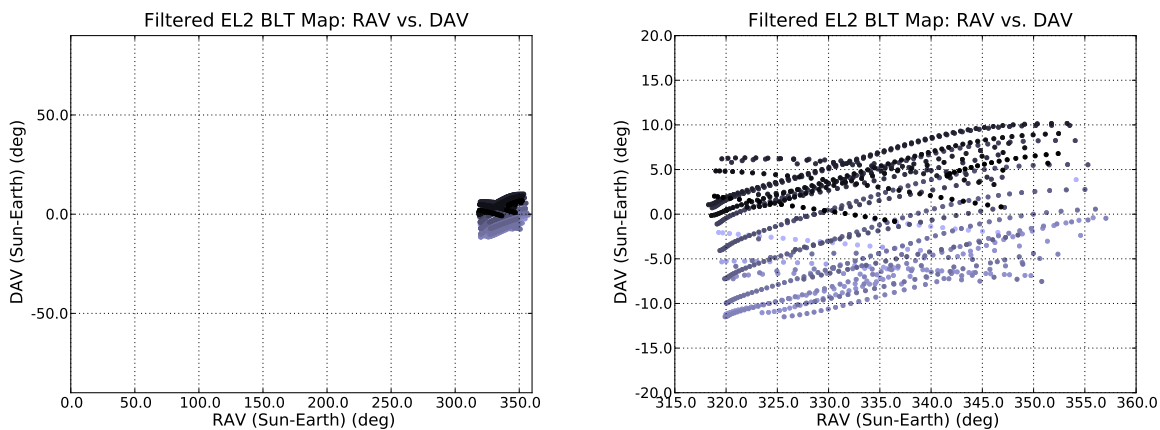


Figure 17. The same relationship between RAV and DAV as Figure 16, but for the filtered EL_2 transfers.

A relationship has also been observed between the injection RAV value and the injection C3. Figure 19 shows this relationship for both the EL_1 and EL_2 transfers. One can see that higher RAV values require less injection energy and there is very little monthly variation in the observed data.

Another parameter that depends closely on the relative orientation of the Moon's orbit about the Earth at the time of the transfer is the inclination of the LEO parking orbit that is used to transfer onto these

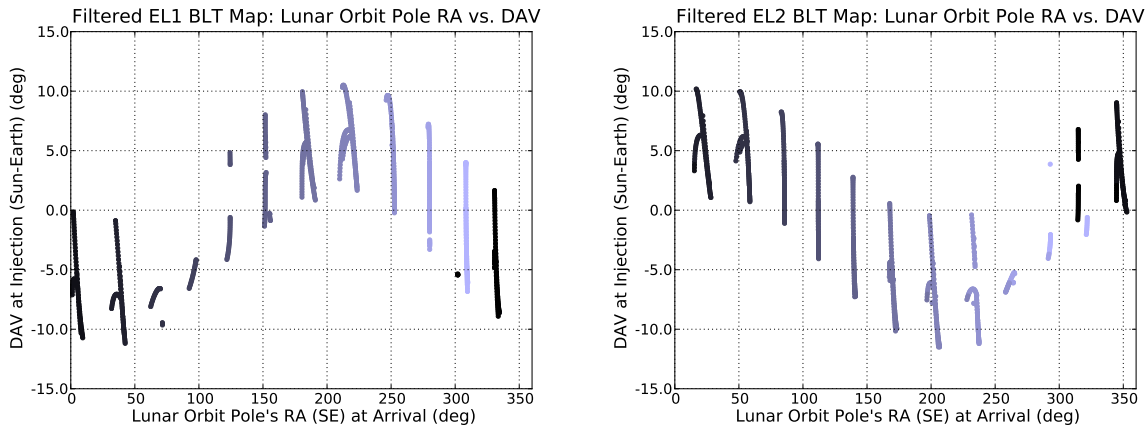


Figure 18. The relationship between the right ascension of the lunar orbit's pole vector at the time of arrival and the value of DAV at the time of injection, both computed in the Sun-Earth rotating coordinate frame. This relationship is shown for each EL₁ (left) and EL₂ (right) transfer in the 12 month survey that satisfies the filter criteria.

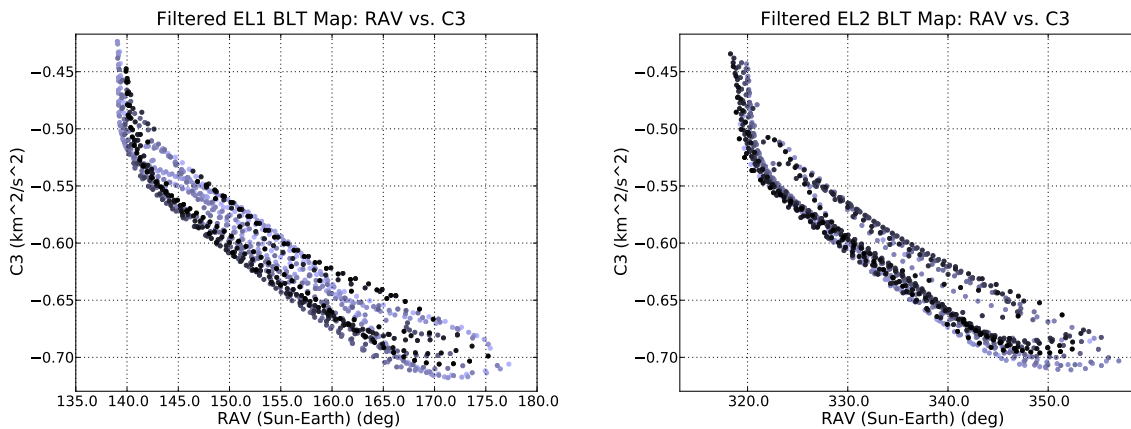


Figure 19. The relationship between the right ascension of the apogee vector, RAV, at the time of trans-lunar injection and the injection energy, C3, for each EL₁ (left) and EL₂ (right) transfer in the 12 month survey that satisfies the filter criteria.

low-energy transfers. The transfers are constructed by building an initial state at the Moon and propagating backward in time until they intersect a 185 km parking orbit above the Earth's surface. The inclination of that parking orbit is driven by the geometry of the transfer. A real mission launched from Cape Canaveral, Florida, would likely launch from an orbit with an equatorial inclination near 28.5° and perform maneuvers to target the desirable low-energy transfer,¹⁵ however, this study is considering only ballistic transfers. Furthermore, it has been shown that the closer the natural transfer is to having a parking orbit with a particular, desired inclination, the less ΔV is required to target that transfer from the desired parking orbit.¹⁵

Figure 20 shows the relationship between the reference date of the lunar halo orbit and the equatorial inclination of the natural LEO parking orbit needed to perform the transfer. One can see that the inclination varies significantly from one month to the next. Figure 21 shows the relationship between the right ascension of the lunar orbit pole vector and the ecliptic inclination of the LEO parking orbit. One can clearly see that there is an evolution of the inclination from one month to the next. Figure 22 shows the same plot, but this time presenting the relationship between the lunar orbit pole vector and the equatorial inclination of the LEO parking orbit.

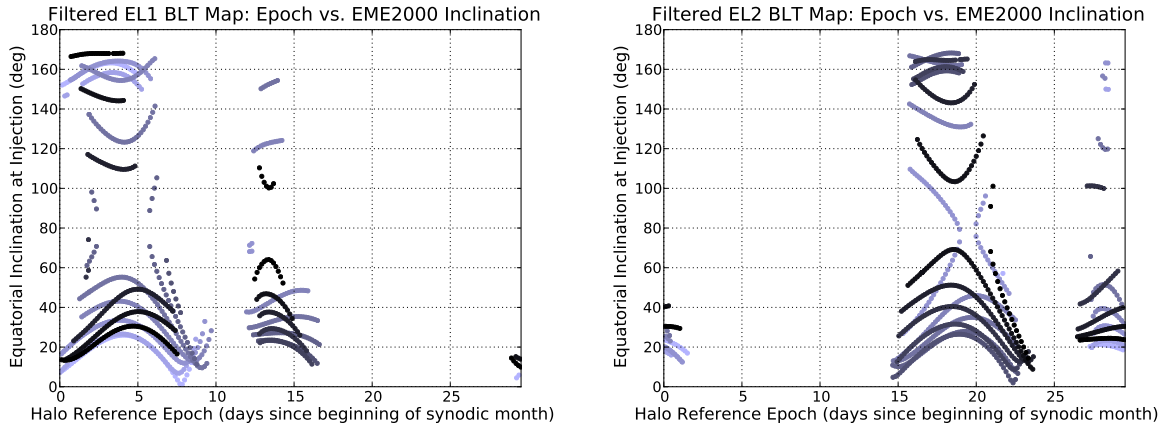


Figure 20. The relationship between the reference date of the lunar halo orbit and the equatorial inclination of the LEO parking orbit needed to perform the transfer. This relationship is shown for each EL_1 (left) and EL_2 (right) transfer in the 12 month survey that satisfies the filter criteria.

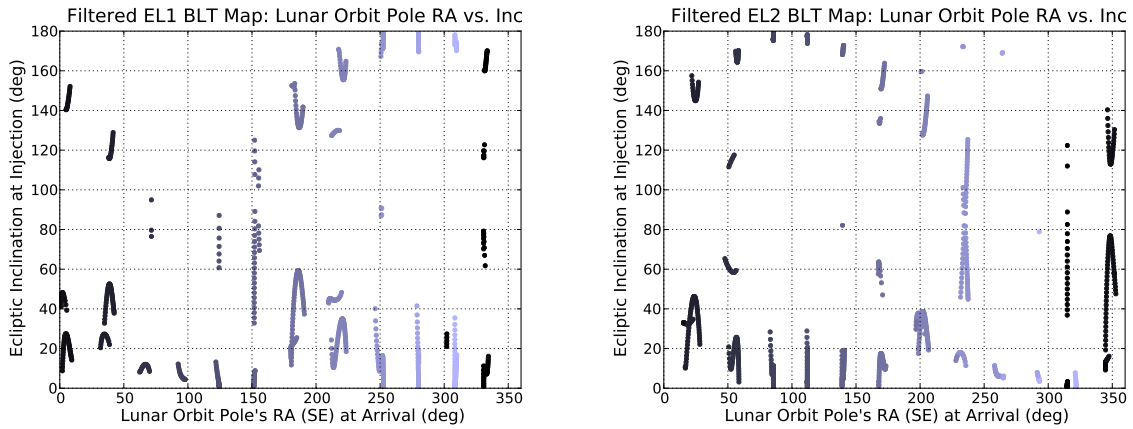


Figure 21. The relationship between the right ascension of the lunar orbit pole vector and the ecliptic inclination of the LEO parking orbit. This relationship is shown for each EL_1 (left) and EL_2 (right) transfer in the 12 month survey that satisfies the filter criteria.

III. Annual Variations

Much of the monthly variation observed in families of low-energy lunar transfers is caused by the Moon's non-circular, inclined orbit relative to the Earth. Other variations in the solar system change over the course of several years. It is therefore of interest to ensure that the relationships observed in this paper hold over the course of several years. The same analyses performed in the previous section have been performed again on a set of transfers constructed with reference dates spanning the year 2021, four years after the previous study. The results of this new study coincide very well with the previous study. Not all of the results will be shown here for brevity.

Figure 23 shows the relationship between T_{ref} and τ , where the lighter shaded points are low-energy transfers that exist in 2017 and the darker points are low-energy transfers that exist in 2021. One can see that the combinations of the two parameters are very similar for both years. Figure 24 shows a similar comparison between the injection C3 and duration of the transfers in both 2017 and 2021. One can see that there is very little noticeable difference between the points in 2017 and 2021.

The transfers that exist in 2021 have been filtered in the same way as the transfers in this study in order to observe how the family might change over the course of four years. Figures 25 and 26 show the same relationships as shown in Figures 18 and 21, except now for filtered transfers in 2017 and 2021. One can see that the 2021 parameters overlap the 2017 data very well, including the dramatic monthly variations

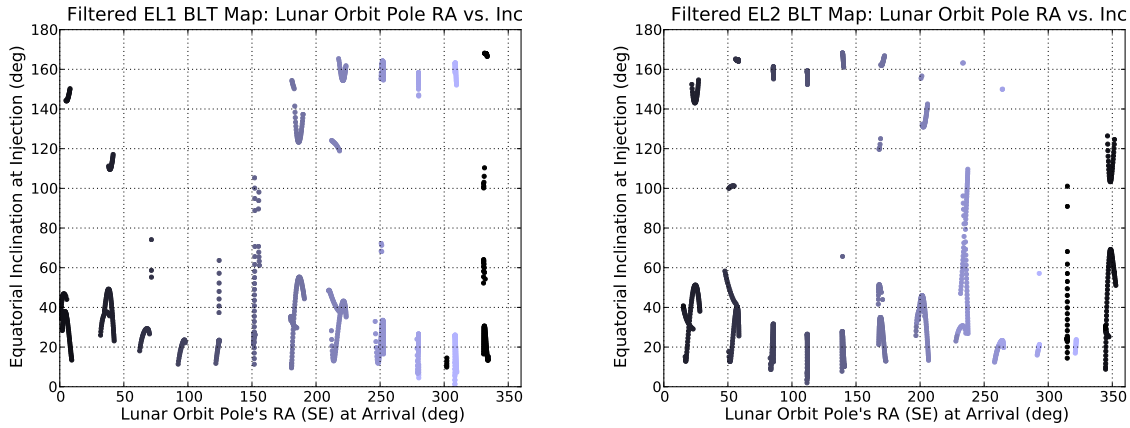


Figure 22. The relationship between the right ascension of the lunar orbit pole vector and the equatorial inclination of the LEO parking orbit. This relationship is shown for each EL_1 (left) and EL_2 (right) transfer in the 12 month survey that satisfies the filter criteria.

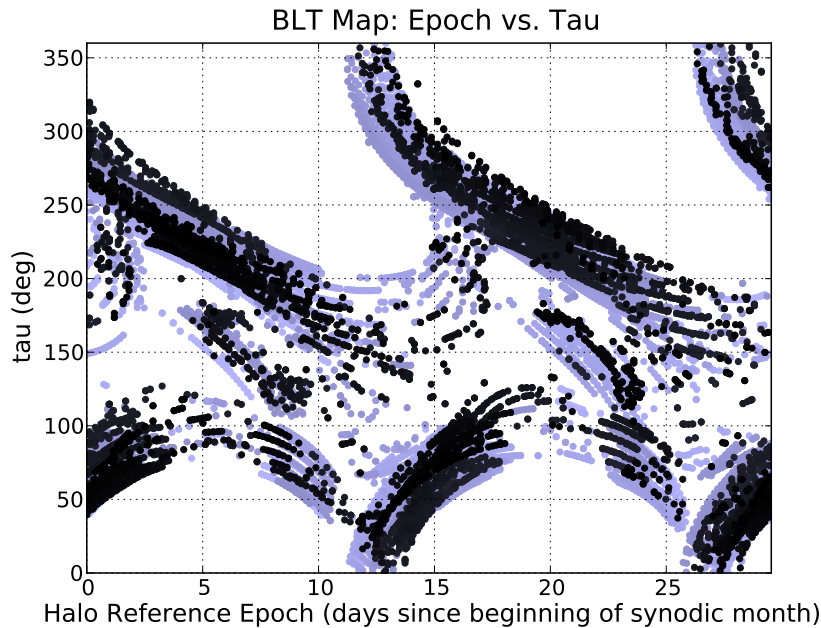


Figure 23. The combinations of T_{ref} and τ that yield low-energy transfers between 185 km LEO parking orbits and the target lunar libration orbit during 2017 (light points) and 2021 (dark points).

observed in the data.

The evidence suggests that the yearly variations are much more subtle than the monthly variations that exist.

IV. Practical Applications

Low-energy lunar transfers are a very different and potentially lower-cost manner for spacecraft to travel to the Moon than conventional lunar transfers. The Artemis and GRAIL spacecraft have already demonstrated the benefits of using low-energy lunar transfers.^{1,22} The two Artemis spacecraft have been able to depart their Earth orbits and transfer to lunar libration orbits using much less fuel than would have been necessary with conventional lunar transfers. Furthermore, the spacecraft did not have enough fuel to make the transition

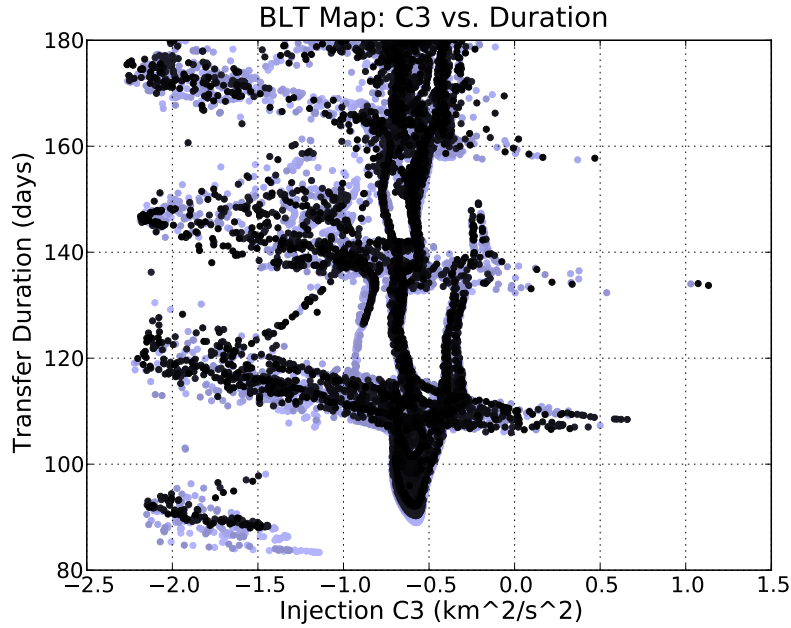


Figure 24. The combinations of injection C3 and transfer duration that yield viable low-energy lunar transfers in 2017 (light points) and 2021 (dark points).

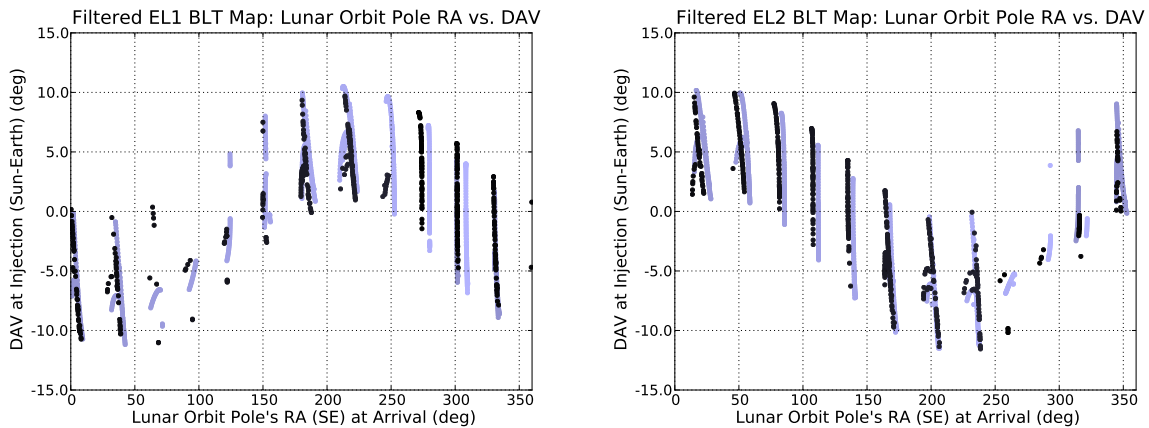


Figure 25. The relationship between the right ascension of the lunar orbit pole vector and the declination of the apogee vector at the time of injection. This relationship is shown for each EL_1 (left) and EL_2 (right) transfer in both the 2017 (light) and 2021 (dark) surveys that satisfies the filter criteria.

without implementing a low-energy lunar transfer. GRAIL has taken advantage of the flexibility of the 3-month low-energy transfer to establish a 21 day launch period: something that is generally not possible with conventional lunar transfers.

The results presented in this paper may be directly applied to missions such as Artemis and GRAIL as their low-energy lunar transfers are being designed. A mission designer can generate better estimates for how a lunar transfer will change if the transfer's departure date changes by one or more months. Furthermore, the results of these surveys provides knowledge about what sorts of low-energy transfers repeat each month, and which only exist in a few months of a year.

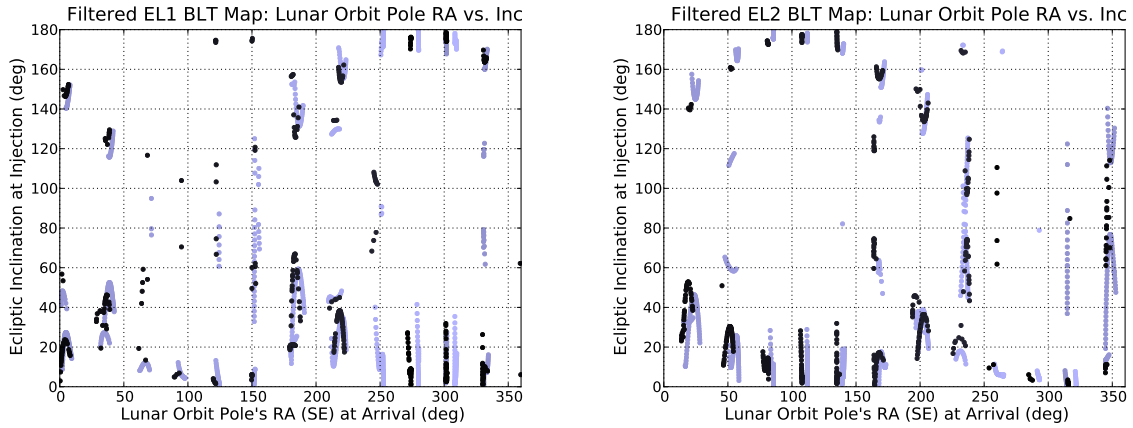


Figure 26. The relationship between the right ascension of the lunar orbit pole vector and the ecliptic inclination of the LEO parking orbit. This relationship is shown for each EL₁ (left) and EL₂ (right) transfer in both the 2017 (light) and 2021 (dark) surveys that satisfies the filter criteria.

V. Conclusions

This research has studied the monthly variations observed in families of low-energy transfers between the Earth and a specific lunar libration orbit. It has been found that several performance parameters of low-energy transfers have large monthly variations, while others remain nearly immutable to such variations. Furthermore, some families of transfers exist only in certain months of the year; these transfers typically involve a sequence of lunar flybys or Earth phasing orbits that are sensitive to geometry shifts.

The relationships studied in this paper are specific to low-energy transfers to a specific target orbit. It would be useful to verify that these relationships persist with other target orbits as well. Nevertheless, several conclusions may be drawn from this specific study and they may certainly be applicable to similar transfer problems.

It has been found that the relationships between the injection energy of the families of low-energy transfers and the closest approach that they make with the Moon are not sensitive to monthly variations, at least for simple transfers that involve no lunar flybys or Earth phasing orbits. The relationship between injection energy and transfer duration is also not very sensitive to variations in the geometry from one month to the next for simple lunar transfers. The monthly variations of complex lunar transfers have not been fully characterized yet.

The departure geometry has been found to be very predictable when observed in the Sun-Earth rotating coordinate frame. It has been found that a family of transfers has a small range of RAV and DAV values in the Sun-Earth rotating frame. There is a dependency on the declination of the apogee vector to the time of the year of the transfer mostly due to the out of plane components of the Moon's orbit about the Earth relative to the ecliptic. An inverse relationship has been identified between the value of the departure's RAV and its injection energy. In addition, it has been observed that the natural inclination of the departure depends significantly on the month of the year of the transfer's departure.

This study investigated the annual variations in a family of transfers as well as the monthly variations and determined that the annual variations are much less pronounced than the monthly variations. The parameters of an example family of transfers matched very closely when comparing their values in 2017 with their values four years later.

Acknowledgements

The research presented in this paper has been carried out at the Jet Propulsion Laboratory, California Institute of Technology, under a contract with the National Aeronautics and Space Administration.

References

- ¹S. B. Broschart, M. J. Chung, S. J. Hatch, J. H. Ma, T. H. Sweetser, S. S. Weinstein-Weiss, and V. Angelopoulos, "Preliminary Trajectory Design for the Artemis Lunar Mission," *AAS/AIAA Astrodynamics Specialist Conference*, No. AAS 09-382, Pittsburgh, Pennsylvania, AAS/AIAA, August 9–13, 2009.
- ²C. Conley, "Low Energy Transit Orbits in the Restricted Three Body Problem," *SIAM Journal Appl. Math.*, Vol. 16, No. 4, 1968, pp. 732–746.
- ³J. S. Parker, *Low-Energy Ballistic Lunar Transfers*. PhD thesis, University of Colorado, Boulder, Colorado, 2007.
- ⁴J. S. Parker and G. H. Born, "Modeling a Low-Energy Ballistic Lunar Transfer Using Dynamical Systems Theory," *Journal of Spacecraft and Rockets*, Vol. 45, No. 6, 2008, pp. 1269–1281.
- ⁵J. S. Parker, "Low-Energy Ballistic Transfers to Lunar Halo Orbits," *AAS/AIAA Astrodynamics Specialist Conference*, No. AAS 09-443, Pittsburgh, Pennsylvania, AAS/AIAA, August 9–13, 2009.
- ⁶W. S. Koon, M. W. Lo, J. E. Marsden, and S. D. Ross, "Shoot the Moon," *AAS/AIAA Spaceflight Mechanics 2000*, Vol. 105, part 2, AAS/AIAA, 2000, pp. 1017–1030.
- ⁷E. A. Belbruno and J. Miller, "A Ballistic Lunar Capture Trajectory for the Japanese Spacecraft Hiten," Tech. Rep. IOM 312/90.4-1731-EAB, JPL, California Institute of Technology, 1990.
- ⁸E. A. Belbruno, "Lunar Capture Orbits, a Method of Constructing Earth Moon Trajectories and the Lunar Gas Mission," *The 19th AIAA/DGLR/JSASS International Electric Propulsion Conference*, No. AIAA 87-1054, Colorado Springs, Colorado, May 1987.
- ⁹E. A. Belbruno, *Capture Dynamics and Chaotic Motions in Celestial Mechanics*. Princeton University Press, Princeton, NJ, 2004.
- ¹⁰V. V. Ivashkin, "On Trajectories of the Earth-Moon Flight of a Particle with its Temporary Capture by the Moon," *Doklady Physics, Mechanics*, Vol. 47, No. 11, 2002, pp. 825–827.
- ¹¹V. V. Ivashkin, "On the Earth-to-Moon Trajectories with Temporary Capture of a Particle by the Moon," *54th International Astronautical Congress*, No. Paper IAC-03-A.P.01, Bremen, Germany, Sept. 29–Oct. 3, 2003, pp. 1–9.
- ¹²V. V. Ivashkin, "On Particle's Trajectories of Moon-to-Earth Space Flights with the Gravitational Escape from the Lunar Attraction," *Doklady Physics, Mechanics*, Vol. 49, No. 9, 2004, pp. 539–542.
- ¹³J. S. Parker and M. W. Lo, "Shoot the Moon 3D," *AAS/AIAA Astrodynamics Specialist Conference*, No. AAS 05-383, Lake Tahoe, CA, AAS/AIAA, August 7–11, 2005.
- ¹⁴J. S. Parker, "Families of Low-Energy Lunar Halo Transfers," *AAS/AIAA Spaceflight Dynamics Conference*, No. AAS 06-132, Tampa, FL, AAS/AIAA, January 22–26, 2006.
- ¹⁵J. S. Parker, "Targeting Low-Energy Ballistic Lunar Transfers," *AAS, George H. Born Special Symposium*, No. AAS 09-443, Boulder, Colorado, AAS, May 13–14, 2010.
- ¹⁶K. C. Howell, "Three-Dimensional, Periodic, 'Halo' Orbits," *Celes. Mech.*, Vol. 32, No. 1, 1984, pp. 53–71.
- ¹⁷V. Szebehely, *Theory of Orbits: The Restricted Problem of Three Bodies*. New York: Academic Press, 1967.
- ¹⁸G. Gómez, J. Masdemont, and C. Simó, "Quasihalo Orbits Associated with Libration Points," *The Journal of the Astronautical Sciences*, Vol. 46, No. 2, 1998, pp. 135–176.
- ¹⁹R. Wilson, "Derivation of Differential Correctors Used in GENESIS Mission Design," Tech. Rep. JPL IOM 312.I-03-002, Jet Propulsion Laboratory, California Institute of Technology, 2003.
- ²⁰K. C. Howell and H. J. Pernicka, "Numerical Determination of Lissajous Trajectories in the Restricted Three-Body Problem," *Celes. Mech.*, Vol. 41, 1988, pp. 107–124.
- ²¹W. M. Folkner, J. G. Williams, and D. H. Boggs, "The Planetary and Lunar Ephemeris DE 421," Tech. Rep. IOM 343R-08-003, Jet Propulsion Laboratory, California Institute of Technology, March 2008. ftp://naif.jpl.nasa.gov/pub/naif/generic_kernels/spk/planets/de421_announcement.pdf.
- ²²P. Xaypraseuth, "Gravity Recovery and Interior Laboratory (GRAIL) Project: Mission Plan," Tech. Rep. JPL D-38928, JPL, California Institute of Technology, 4800 Oak Grove Dr., Pasadena, CA 91109, November 2008.